available at www.sciencedirect.com

ScienceDirect

journal homepage: www.elsevier.com/locate/biochempharm

Advanced glycation endproducts induce a proliferative response in vascular smooth muscle cells via altered calcium signaling

Kanola C. David, Roderick H. Scott, Graeme F. Nixon *

School of Medical Sciences, University of Aberdeen, Foresterhill, Aberdeen AB25 2ZD, UK

ARTICLE INFO

Article history:
Received 20 June 2008
Accepted 7 August 2008

Keywords:
Vascular smooth muscle
Diabetes
Calcium
Proliferation
Glycation

ABSTRACT

Advanced glycation endproducts (AGEs) are proteins that accumulate in the plasma of diabetics as a result of increased glucose concentrations and are closely linked with vascular disease. The mechanisms involved are still not clear. The aim of this study was to investigate whether AGE-induced changes in calcium (Ca^{2+}) homeostasis could contribute to these mechanisms. Cultured porcine coronary artery vascular smooth muscle (VSM) cells were preincubated with glycated albumin for 96 h. The sphingosine 1-phosphate (S1P)-induced intracellular Ca^{2+} increase, although not increased in amplitude, was significantly prolonged in cells preincubated with glycated albumin. Intracellular Ca^{2+} imaging and electrophysiological recording of ion channel currents following release of caged Ca^{2+} indicated that this prolonged Ca^{2+} rise occurred predominantly via changes in Ca^{2+}-induced Ca^{2+} release. Preincubation with glycated albumin also resulted in a threefold increase in expression of the receptor for AGE. As a consequence of the prolonged intracellular Ca^{2+} rise following preincubation with glycated albumin, the S1P-induced activation of the Ca^{2+}-dependent phosphatase, calcineurin (CaN) was increased. This resulted in increased S1P-induced activation of the Ca^{2+}-dependent transcription factor, nuclear factor of activated T cells (NFATc). BrdU incorporation in VSM cells was increased in cells preincubated with glycated albumin and was inhibited by the CaN inhibitor, cyclosporin A. In conclusion, AGE can induce VSM proliferation via a prolonged agonist-induced Ca^{2+} increase leading to increased activation of CaN and subsequently NFATc. This mechanism may contribute to pathogenesis of vascular disease in diabetes mellitus.

1. Introduction

Diabetes mellitus is a disease characterized by chronic hyperglycaemia due to a deficiency in insulin action. Hyperglycaemia is the primary factor that initiates vascular complications associated with diabetes such as nephropathy, retinopathy and the development of atherosclerosis [1–3]. Based on experimental evidence, several hypotheses have been suggested which could link hyperglycaemia to diabetic vascular complications [4–9]. In recent years, much research has focussed on a mechanism intimately linked with vascular complications, and is also the direct result of hyperglycaemia. Evidence now suggests that many of the vascular complications of diabetes may be mediated by advanced glycation endproducts (AGEs) [10–12]. AGEs are modifications of proteins and lipids that become nonenzymatically glycated and oxidized after contact with sugars [13]. The AGE formation begins with covalent binding of aldehyde or ketone groups of

* *Corresponding author*. Tel.: +44 1224 555854; fax: +44 1224 555754.
E-mail address: g.f.nixon@abdn.ac.uk (G.F. Nixon).
0006-2952/$ – see front matter © 2008 Elsevier Inc. All rights reserved.
doi:10.1016/j.bcp.2008.08.011

reducing sugars, such as glucose, to free amino acid groups of proteins. This undergoes rearrangement to ketoamines (Amadori's product) with highly reactive carbonyl groups (formed as a result of carbonyl stress) [14,15]. These intermediates accumulate and react with various functional protein groups leading to the formation of stable AGE compounds [15]. AGEs, once formed, are mostly irreversible. A crucial factor in the formation of AGEs is the degree of hyperglycaemia [16,17]. Therefore, in diabetes, the intracellular formation of AGEs is greatly increased [16–18]. The importance of AGE in the pathogenesis of diabetic vascular complications is demonstrated by several studies showing AGE inhibitors can reduce microvascular damage in retina, kidney and nerve [19,20]. AGEs are also enriched in atherosclerotic lesions in both human diabetes [21] and in animal models of diabetes [22]. In addition, AGEs can induce vascular smooth muscle (VSM) cell proliferation *in vitro* [23,24] although the mechanisms of this are not clear.

Recently, the potential pathophysiological relevance of circulating AGEs was indicated by the discovery of the receptor for advanced glycation endproducts (RAGE) [25]. RAGE is a multi-ligand member of the immunoglobulin superfamily containing a single transmembrane spanning domain and is expressed in a variety of cell types, including endothelial and VSM cells [26]. Apart from AGEs, other endogenous ligands for RAGE include amphoterin and S100/calgranulin proteins [27]. In addition to the full-length form of RAGE, truncated forms have also been identified with both C- and N-terminal truncations [28]. Only C-terminal truncations and full-length RAGE forms can bind AGEs [28]. RAGE is typically expressed at low levels in cells and may be upregulated in certain conditions [25]. Intracellular pathways stimulated following RAGE engagement with ligand are predominantly those involved in inflammatory responses [29]. RAGE signaling results in activation of a number of pathways, such as mitogen-activated protein (MAP) kinases (extracellular regulated signal kinase (ERK)1/2 and p38MAP kinase), and the small GTPases CDC42, Rac and Ras [30]. In endothelial cells this can result in the activation of the proinflammatory transcription factor, nuclear factor κB (NFκB) [31]. In VSM cells, the RAGE-activated signaling pathways are less clear although activation of Ras, ERK1/2 and NFκB has been previously demonstrated [24,32]. Key studies have now revealed the importance of RAGE in the pathogenesis of atherosclerosis in diabetes [21]. In animal models such as apolipoprotein E knockout mice treated with streptozotocin, blockade of RAGE significantly reduced the formation of atherosclerotic lesions [33]. RAGE knockout transgenic mice also displayed a decreased arterial restenosis following arterial injury compared to wild type mice [34].

An important factor regulating VSM cell phenotype is Ca^{2+}-dependent signaling. Ca^{2+}-dependent transcription factors can play a critical role in modulation of VSM phenotype [35–37]. In cardiac myocytes, AGEs have been reported to alter Ca^{2+} homeostasis [38] although this has not been examined in VSM cells. In the current study the effects of glycated albumin (an AGE found *in vivo*) on agonist-induced Ca^{2+} homeostasis were examined. Preincubation with AGEs for 96 h resulted in a prolonged increase in agonist-induced intracellular Ca^{2+} due, in part, to increased Ca^{2+}-induced Ca^{2+} release (CICR). This leads to increased activation of the Ca^{2+}-dependent phosphatase, calcineurin (CaN). This subsequently results in an activation of the Ca^{2+}-dependent transcription factor, nuclear factor of activated T-cells (NFATc) and increases cell proliferation.

2. Materials and methods

2.1. Primary cell culture

Adult male pig hearts were obtained from a local abattoir and immediately placed in Hanks balanced salt solution. The left descending coronary artery was dissected, connective tissue removed and the endothelium denuded. Arteries were incubated in serum-free Dulbecco's modified Eagle's medium (DMEM) containing 1 mg/ml collagenase (type II), 0.2 mg/ml elastase (type IV) and 50 μg/ml soybean trypsin inhibitor at 37 °C. The tissue was titurated every 30 min until complete dispersal had occurred (3–4 h), transferred to an 80 cm^2 tissue culture flask containing DMEM, 20% foetal bovine serum (FBS), 2 mM L-glutamine, penicillin (10,000 units/ml) and streptomycin (10 mg/ml) and incubated at 37 °C, in a humidified 5% CO_2 atmosphere. After 24 h, the medium was removed and cells transferred to fresh DMEM, 10% FBS, 2 mM L-glutamine, penicillin (10,000 units/ml) and streptomycin (10 mg/ml). Cells were used for experiments between passages 4 and 8. The *n* values given in Figs. 1–3 represent individual measurements from primary cultured single cells derived from at least three different animals.

2.2. Imaging of $[Ca^{2+}]_i$

Cultured VSM cells were grown on glass-bottomed dishes and serum-starved 24 h before use. Cells were loaded with 4 μmol/l Fura-2 AM for 30 min in a solution containing (in mmol/l): 130 NaCl, 5.6 KCl, 1 $MgCl_2$, 1.7 $CaCl_2$, 11 Glucose, 10 HEPES (pH 7.4) followed by a 20 min de-esterification period. A Zeiss Axiovert 200 inverted microscope, equipped with a cooled CCD camera (Photometrics, Tucson, AZ) and a polychromatic illumination system (T.I.L.L. Photonics, Gräfelfing, Germany), was used to capture fluorescence images with excitations at 340 and 380 nm. The ratio of the fluorescence intensity between the pair of frames (FR340/380) was calculated after background subtraction. The Metafluor software (Molecular Devices, PA) controlled the illuminator and camera, and performed image ratio measurements and analysis. Results are expressed as F340/380 ratio. Experiments were carried out at room temperature (22–24 °C).

2.3. Electrophysiology

The whole cell variant of the patch clamp technique was used to record ion channel currents from cultured VSM cells. Patch pipettes (resistances 5–9 MΩ) were filled with a KCl-based solution containing (in mmol/l) 140 KCl, 0.1 $CaCl_2$, 2 $MgCl_2$, 5 EGTA, 10 HEPES, 2 ATP (310–320 mOsm/l and pH 7.2). Recordings were made with extracellular solutions that contained (in mmol/l) 3 KCl, 0.6 $MgCl_2$, 2 $CaCl_2$, 1 $NaHCO_3$, 10 HEPES, 5 glucose and 130 NaSCN (310–320 mOsm/l and pH

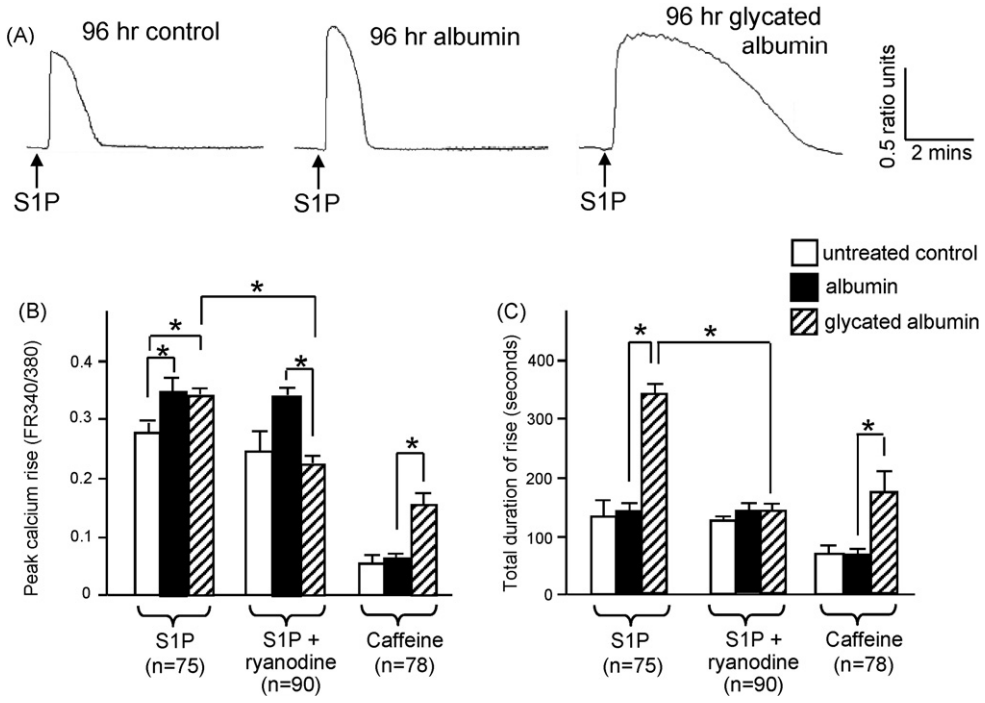

Fig. 1 – Effects of AGE incubation on agonist-induced Ca^{2+} increases in cultured VSM cells. Cells were preincubated for 96 h either untreated, with 200 μg/ml albumin or 200 μg/ml glycated albumin. Intracellular Ca^{2+} was measured in cells following stimulation with 5 μM S1P. (A) Typical S1P-induced increases in $[Ca^{2+}]_i$ are shown. (B) Mean peak Ca^{2+} rises following stimulation with S1P alone and S1P in the presence of 10 μM ryanodine. Mean peak Ca^{2+} rises induced by 20 mM caffeine are also shown. (C) Mean data of the total duration for Ca^{2+} rises induced by S1P alone and S1P in the presence of 10 μM ryanodine. Total duration for caffeine-induced Ca^{2+} rise is also shown. In cells preincubated for 96 h with glycated albumin, ryanodine significantly decreased the prolonged duration and peak of the S1P-induced Ca^{2+} increase to control levels. In cells preincubated with glycated albumin, the caffeine-induced increase in $[Ca^{2+}]_i$ was significantly increased in peak amplitude and duration compared to both untreated control cells and cells preincubated with albumin. *n* numbers shown in brackets, $^*p < 0.05$. All values mean ± S.E.M.

7.4). VSM cells were recorded using NaSCN-based extracellular solution because the success rate of seal formation and whole cell recording under these conditions was greatly improved. Whole cell currents were measured using an Axoclamp 2A amplifier (Molecular Devices, CA) operated at 18 kHz. Drugs were applied by low-pressure perfusion from a blunted pipette positioned ~50 μm from the cell being studied. Current/voltage relationships were generated from a holding potential of −70 mV by step depolarisations to clamp potentials between −60 and +130 mV. Hyperpolarizing step commands of −50 mV were used for linear leak subtraction. Data were stored on digital audiotape using a digital tape recorder (DTR 1205, Biologic) and subsequently analysed off-line with CED voltage clamp software.

Intracellular flash photolysis of caged compounds (ATP, inositol 1,4,5-trisphosphate (IP_3) and DM-nitrophen; Calbiochem, Nottingham, UK) was conducted as previously reported [39]. Briefly, where stated caged compounds were included in the patch pipette solution, ATP and IP_3 at 100 μM and DM-nitrophen at 8 mM (with 4 mM $CaCl_2$). After 5 min equilibrium in the whole cell recording configuration intracellular photolysis was achieved with a flash of intense near UV light from a Xenon flash lamp with UG11 filter attached (Hi-Tech XF-10).

2.4. *Calcineurin activity*

Measurement of calcineurin activation using a colorimetric assay was carried out according to manufacturer's instructions (Calbiochem, Nottingham, UK). Calcineurin activity was determined by dephosphorylation of a phosphopeptide substrate and quantified by comparing to a standard curve with known concentrations of free phosphate. Briefly, cultured VSM cells were grown to 80% confluence in 96-well plates and deprived of serum for 24 h prior to treatment. Following treatment protocols, cells were washed twice in ice cold TBS and lysed with lysis buffer followed by scraping into Eppendorf tubes. Samples were then centrifuged in an ultracentrifuge at 100,000 × *g*, 4 °C for 45 min and the supernatant reserved. Samples were run through a resin-filled column to remove free phosphate. Activity was assessed in each sample in the presence of exogenously added calmodulin, the phosphopeptide substrate and the colorimetric dye. Absorbance was assessed at 620 nm in a spectrophotometer. In parallel, calcineurin activity was also measured in samples in the presence of 10 mM EGTA to determine the phosphatase activity due to calcium-independent phosphatases. For each sample, the phosphatase activity in the presence of EGTA was

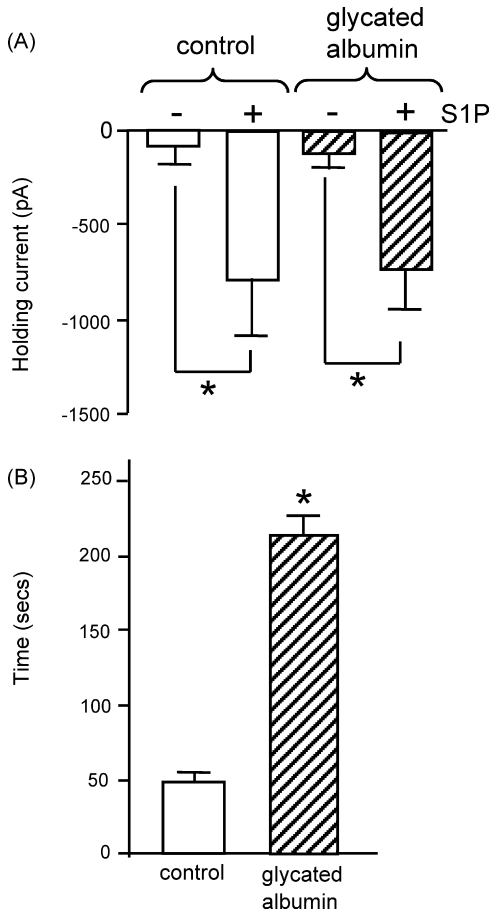

Fig. 2 – S1P-activated inward currents in control and AGE-treated VSM cells. (A) Bar chart showing mean ± S.E.M. values for the holding currents recorded prior to S1P application and during the peak of the 1 μM S1P response. Data are given for control cells ($n = 6$) and cells preincubated with 200 μg/ml glycated albumin for 96 h ($n = 5$). (B) S1P response duration from control ($n = 3$) and glycated albumin-treated ($n = 3$) VSM cells. All data were obtained from cells bathed in NaSCN-based extracellular solution and clamped at a holding voltage of −70 mV. $^*p < 0.05$.

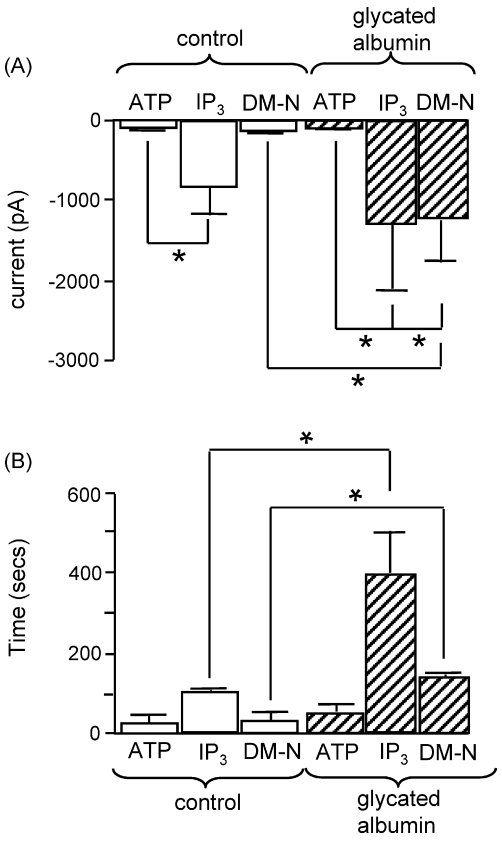

Fig. 3 – AGE preincubation of VSM cells prolonged responses to intracellular photorelease of IP_3 and DN-nitrophen. (A) Graph showing mean values for the peak inward currents evoked by intracellular photorelease of caged ATP, caged IP_3 and caged Ca^{2+} (DM-nitrophen, DM-N). $n = 3$ for each group. Whereas photorelease of IP_3 was not significantly different in AGE-treated and control cells, photorelease of Ca^{2+} significantly increased inward current in following AGE-preincubation. (B) Bar chart showing the mean ± S.E.M. values for inward current durations recorded from control ($n = 3$) and AGE-treated ($n = 3$) VSM cells following intracellular photorelease of caged ATP, caged IP_3 and caged Ca^{2+} (DM-nitrophen, DM-N), $^*p < 0.05$. All data were obtained from cells bathed in NaSCN-based extracellular solution and clamped at a holding voltage of −70 mV.

subtracted from total activity to determine the phosphatase activity due to calcineurin. Results were expressed as nmoles phosphate released based on comparison with the standard curve. Each individual assay comprised of treated samples and a standard curve.

2.5. *Electromobility shift assay*

EMSA were carried out as previously described [37]. Briefly, cultured pig coronary artery VSM cells were treated as appropriate and nuclear fractions were prepared. 10 μg of protein from nuclear preparations was used in each experiment. Biotin-labelled consensus oligonucleotides for the transcription factor NFAT (5′-ACGCCCAAAGAGGAAAATTT-GTTTCATACA) were incubated with nuclear fractions according to the manufacturer's instructions (Panomics, Fremont, CA). For competition experiments, unlabelled probe was added in addition to the biotin-labelled probe. Protein–DNA complexes were resolved on a 6% polyacrylamide gel. Bands were visualized using a streptavidin-HRP detection reagent as per manufacturer's instructions. Shifted bands were quantified by scanning densitometry using a Bio-Rad GS-690 imaging densitometer.

2.6. *Bromodeoxyuridine assay*

DNA synthesis as a measure of cell proliferation was determined by assessing BrdU incorporation into VSM cells. Briefly, cultured VSM cells were grown to 80% confluence in 96-well plates and deprived of serum for 24 h prior to

treatment. Following treatment, BrdU label was added to cells according to manufacturer's instructions (Calbiochem, Nottingham, UK). Regardless of treatment incubation times, BrdU incubation was included for the last 24 h before analysis. Each assay also included a blank (no cells) and a background sample (cells, no BrdU added). Cells were fixed in fixative/denaturing solution for 30 min and anti-BrdU antibody was added each well for 1 h at room temperature. Cells were washed three times with wash buffer. The horseradish peroxidase (HRP) conjugated antibody was added to each well for 30 min at room temperature. Wells were washed three times and substrate solution (tetra-methylbenzidine) added. Absorbance in each well was measured using a spectrophotometric plate reader at wavelengths of 450 and 595 nm.

2.7. SDS-polyacrylamide gel electrophoresis and immunoblotting

Cultured coronary artery VSM cells were grown to 90% confluence and deprived of serum for 24 h prior to treatment as indicated. Cells were lysed in lysis buffer and cellular debris removed by centrifugation at 15,000 × *g* for 15 min at 4 °C, prior to analysis by immunoblotting. Cell lysates were mixed with an equal volume of 2× SDS sample buffer and incubated at 100 °C for 5 min. Lysates were fractionated by SDS-PAGE and transferred to nitrocellulose membranes. After blocking with 5% nonfat milk powder in TBS, pH 7.4, containing 0.1% Tween-20 for 1 h at room temperature, blots were incubated with anti-RAGE antibody (Santa Cruz, CA) for 1 h at room temperature or overnight at 4 °C, washed and incubated with HRP-conjugated anti-rabbit secondary antibody (Dako, Glostrup, Denmark) for 1 h at room temperature. Immuno-reactive species were visualized using enhanced chemiluminescence and quantitated by scanning densitometry using a Bio-Rad GS-690 imaging densitometer.

2.8. Materials

All chemicals and reagents (including glycated bovine albumin and corresponding control bovine albumin (non-glycated)) were purchased from Sigma Chemical Co., Dorset, UK, unless otherwise stated. The degree of substitution on all batches of glycated albumin was the same (2.7 mol hexose per mole albumin). Results were confirmed with another source of glycated albumin from Calbiochem with a similar degree of substitution.

2.9. Statistical analyses

Data are expressed as mean ± S.E.M. Significance was tested using a Student's *t*-test or, where multiple comparisons were required, two-way ANOVA. A value of $p < 0.05$ was considered significant.

3. Results

3.1. Effects of glycated albumin on agonist-induced $[Ca^{2+}]_i$

In order to mimic the effects of AGE *in vivo*, cells were incubated for 96 h with 200 μg/ml of glycated bovine albumin. This concentration has previously been shown *in vitro* to approximate *in vivo* vascular effects of experimentally induced diabetes in pig coronary arteries [40]. In addition, it is within the range of glycated albumin found in plasma [41]. Cultured VSM cells were incubated for 96 h with either 200 μg/ml glycated albumin, 200 μg/ml (non-glycated) albumin or untreated (no added albumin) and the agonist-induced $[Ca^{2+}]_i$ increase was measured in Fura-2 loaded cells. The agonist used in this study was sphingosine 1-phosphate (S1P). We have previously shown that S1P induces an increase in $[Ca^{2+}]_i$ in VSM cells predominantly via a release of Ca^{2+} from intracellular stores [42]. In control VSM cells (no added albumin), 5 μM S1P induced a transient Ca^{2+} rise (Fig. 1A). S1P also produced an increase in $[Ca^{2+}]_i$ in cells incubated for 96 h with albumin. There was a small but significant increase in the peak rise compared to untreated cells (Fig. 1B). The duration of the transient increase was similar (Fig. 1C). In VSM cells incubated with glycated albumin for 96 h, S1P produced an increase in $[Ca^{2+}]_i$ which was not significantly different in amplitude from cells incubated with albumin (Fig. 1B). However, the duration of this Ca^{2+} rise (total time from initial rise until return to baseline) was significantly prolonged compared to both untreated and albumin-treated cells (Fig. 1C). VSM cells incubated with glycated albumin for 24 and 48 h did not reveal an increased S1P-induced Ca^{2+} increase. Cells incubated for 72 h with glycated albumin did have an increased duration for S1P-induced Ca^{2+} increase but this was significantly less than that obtained for the 96 h incubation (data not shown).

In order to investigate potential mechanisms for the prolonged S1P-induced Ca^{2+} rise following AGE incubation, VSM cells were incubated for 96 h with 200 μg/ml glycated albumin, 200 μg/ml albumin or untreated. 10 μM ryanodine was added for 30 min to block ryanodine receptors (RyR) before stimulation of a Ca^{2+} increase with S1P. Following ryanodine incubation, the magnitude of the S1P-induced Ca^{2+} increase was unchanged in untreated VSM cells and in cells pre-incubated with albumin. In VSM cells preincubated with glycated albumin for 96 h, ryanodine significantly reduced the peak Ca^{2+} rise induced by S1P (Fig. 1). The duration of the S1P-induced Ca^{2+} rise was unchanged in the presence of ryanodine for untreated cells and for cells preincubated with albumin. However, in cells preincubated with glycated albumin, ryanodine significantly reduced the prolonged duration of the S1P-induced Ca^{2+} increase back to the duration of untreated cells (Fig. 1C).

As the 96 h pre-incubation with AGE may have effects on RyR which result in a prolonged agonist-induced Ca^{2+} increase, the ability of caffeine to activate RyR in VSM cells was investigated. Following pre-incubation with either 200 μg/ml glycated albumin or 200 μg/ml albumin, VSM cells were stimulated with 20 mM caffeine and the effects on $[Ca^{2+}]_i$ determined. Caffeine produced a rise in $[Ca^{2+}]_i$ in cells regardless of pre-incubation treatment. There was no significant difference between untreated and albumin-treated cells. In cells pre-incubated with glycated albumin, the caffeine-induced Ca^{2+} rise was significantly greater in amplitude and more prolonged in duration compared to cells pre-incubated with albumin (Fig. 1B and C).

3.2. Effects of glycated albumin on membrane currents

S1P (1 μM) activated inward currents of similar magnitudes in both control and glycated albumin-treated VSM cells bathed in NaSCN solution (Fig. 2). Fig. 2A shows the mean data for the holding current at the resting holding potential of −70 mV and the subsequent increase in inward current evoked by S1P. Although the peak amplitudes of the responses to S1P were not significantly different in control compared to cells preincubated with glycated albumin, the durations of the responses were significantly longer in preincubated cells (Fig. 2B) in agreement with Ca^{2+} imaging experiments.

To further investigate the roles of IP_3 in S1P responses of VSM cells caged IP_3 was photoreleased inside control and AGE-treated cells. Initially control experiments were conducted using caged ATP to consider the effects of the flash and by-products of photolysis. Intracellular photorelease of ~10 μM ATP produced delayed, short and small inward currents. In contrast at least 10 times larger inward currents were evoked by intracellular photorelease of ~10 μM IP_3 (Fig. 3A). The peak amplitudes of the responses to intracellular photorelease in control and glycated albumin-treated VSM cells were not significantly different but the duration of the responses recorded were significantly prolonged in cells pre-incubated with glycated albumin compared to control cells (Fig. 3B). Intracellular photorelease of Ca^{2+} from DM-nitrophen evoked inward currents which were significantly larger and longer lasting in VSM cells pre-incubated with glycated albumin compared with control cells (Fig. 3A and B).

3.3. RAGE expression following incubation with AGE in VSM cells

It has previously been reported in some cell types that incubation with AGE can upregulate expression of RAGE. Primary cultured porcine coronary artery VSM cells were pre-incubated with 200 μg/ml albumin or 200 μg/ml glycated albumin for 96 h and RAGE expression determined by immunoblotting with an anti-RAGE antibody. RAGE was expressed in untreated cells and cells preincubated with albumin (Fig. 4A and B). In cells preincubated with glycated albumin, RAGE expression was significantly increased by approximately threefold. To determine whether other signaling pathways may be upregulated, possibly as a result of increased RAGE expression, ERK1/2 phosphorylation was measured in VSM cells following pre-incubation with glycated albumin for 96 h. Neither basal nor S1P-stimulated ERK1/2 phosphorylation was altered as a result of pre-incubation with glycated albumin (Fig. 4C).

3.4. Effects of AGE on calcineurin activity in VSM cells

The Ca^{2+}/calmodulin-dependent protein phosphatase, calcineurin (CaN), is involved in activation of various signaling pathways. CaN has also been shown to directly dephosphorylate the transcription factor NFATc, leading to its activation and translocation to the nucleus [44]. NFATc-induced gene expression has been associated with VSM cell proliferation [45]. Using a phosphosubstrate, the effects of AGE incubation in CaN activity was assessed. Cells were incubated

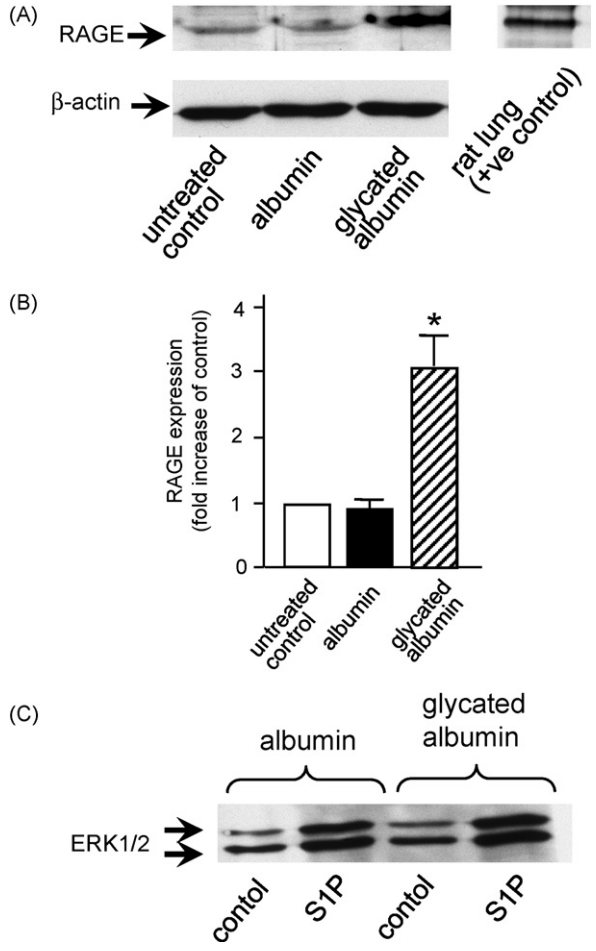

Fig. 4 – RAGE expression and activation of ERK1/2 in VSM cells. Typical immunoblot (A) and mean expression data (B) of RAGE expression in homogenates from primary cultured porcine coronary artery VSM cells. Cells were either untreated, preincubated with 200 μg/ml albumin or 200 μg/ml glycated albumin for 96 h ($n = 4$). (C) S1P-induced phosphorylation of ERK1/2 in cells pre-incubated with either albumin or glycated albumin for 96 h ($n = 3$). *$p < 0.05$.

with either 200 μg/ml glycated albumin or 200 μg/ml albumin for 96 h and stimulated with 5 μM S1P for 30 min. In untreated control cells and in cells preincubated with albumin or glycated albumin, S1P produced a significant increase in CaN activity after 30 min stimulation as assessed by nmoles phosphate released from the phosphosubstrate (Fig. 5A). There was no significant difference between albumin-treated and untreated VSM cells (untreated data not shown). However, VSM cells preincubated with glycated albumin showed a significantly increased resting level of CaN activation and an increased level following S1P stimulation of 30 mins (Fig. 5A).

3.5. NFATc activation following AGE incubation

NFATc activation in VSM was determined by EMSA. VSM cells were preincubated for 96 h with 200 μg/ml albumin or 200 μg/ml glycated albumin and stimulated with 5 μM S1P for 30 min.

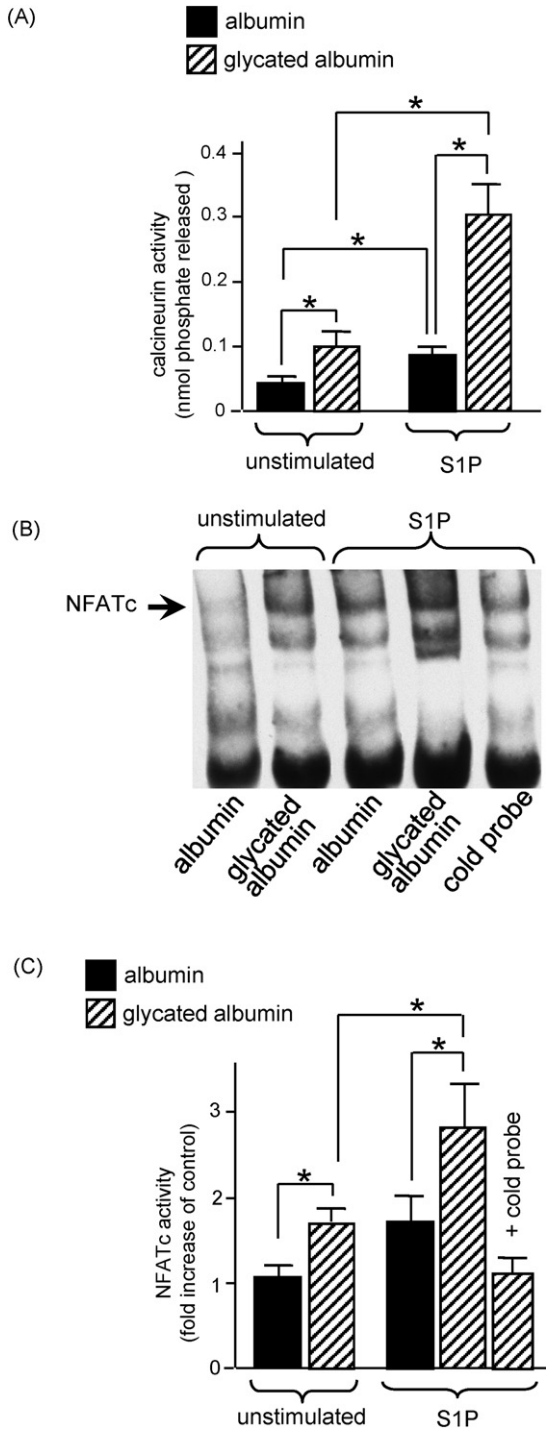

Fig. 5 – Effects of AGE on activity of calcineurin and NFATc in cultured VSM cells. (A) Cells were preincubated for 96 h either untreated (not shown), with 200 μg/ml albumin or 200 μg/ml glycated albumin and calcineurin activity was measured in resting (unstimulated) conditions and following addition of 5 μM S1P for 30 min. $n = 7$ for each group. (B) Nuclear fractions were prepared from cells preincubated for 96 h either untreated (not shown), with 200 μg/ml albumin or 200 μg/ml glycated albumin and NFATc activation was measured in resting (unstimulated) conditions and following addition of 5 μM S1P for 30 min (shifted band is denoted by the arrow). (C) Mean data of NFATc activation expressed as fold increase of control conditions (untreated, unstimulated). $n = 5$ for each group, $^*p < 0.05$.

Following S1P stimulation, NFATc activity was increased in VSM cells regardless of preincubation (Fig. 5B and C). The basal levels and S1P-stimulated levels of NFATc activation were similar in untreated cells compared to cells preincubated with albumin (untreated data not shown). Cells preincubated with glycated albumin had an increased basal level of NFATc activation and also revealed a significantly increased activation following S1P stimulation compared to cells preincubated with albumin. Specificity of the oligonucleotide probes is indicated by the reversal of S1P-stimulated NFATc activation following addition of cold (unlabelled) probe.

3.6. *BrdU incorporation*

It has been previously demonstrated that AGE can enhance proliferation in VSM cells in culture [23,24]. The mechanisms are not clear but may involve increased activation of NFATc, also implicated as having an important role in VSM cell proliferation [45]. BrdU incorporation was used to assess increases in DNA expression and indicate a proliferative response. Cells were either untreated or preincubated for 24, 48, 72 or 96 h with glycated albumin or albumin. In this case, S1P was not added to cells. S1P is already known to be mitogenic in VSM cells and would therefore mask the effects of AGEs on proliferation. After 24, 48 or 72 h, there was no significant difference in BrdU incorporation between albumin and glycated albumin preincubation (Fig. 6A). After 96 h, the levels of BrdU incorporation in VSM cells incubated with glycated albumin was significantly increased compared to cells incubated with albumin (Fig. 6A). As the timecourse of this increase is similar to the changes observed in Ca^{2+} homeostasis, cells were incubated with either albumin or glycated albumin for 96 h in the presence of the selective CaN inhibitor, cyclosporin A (CsA). In cells incubated with 10 μM CsA for 96 h, BrdU incorporation was reduced to zero regardless of preincubation conditions (although a maintained cell viability was assessed by activation of ERK1/2 which was unaffected by CsA incubation, data not shown). To more clearly assess the potential role of an increased CaN activity potentially via an AGE-dependent mechanism, cells were treated with CsA only in the last 24 h, i.e. after 72 h of the total 96 h preincubation with glycated albumin or albumin. The rationale for this is that AGE-induced effects on intracellular Ca^{2+} and CaN were only evident after at least 72 h incubation. This potentially would block more selectively the AGE-induced changes to proliferation. In this case, the VSM cells preincubated with albumin for 96 h and CsA for the final 24 h showed a small significant decrease in BrdU incorporation. However, in cells preincubated with glycated albumin for 96 h, CsA treatment after 72 h significantly reduced the BrdU incorporation to control levels (approximately 80% decrease, Fig. 6A). The treatment of cells with CsA after 72 h incubation did not significantly change BrdU incorporation in cells stimulated with 10% FBS for 96 h (Fig. 5B).

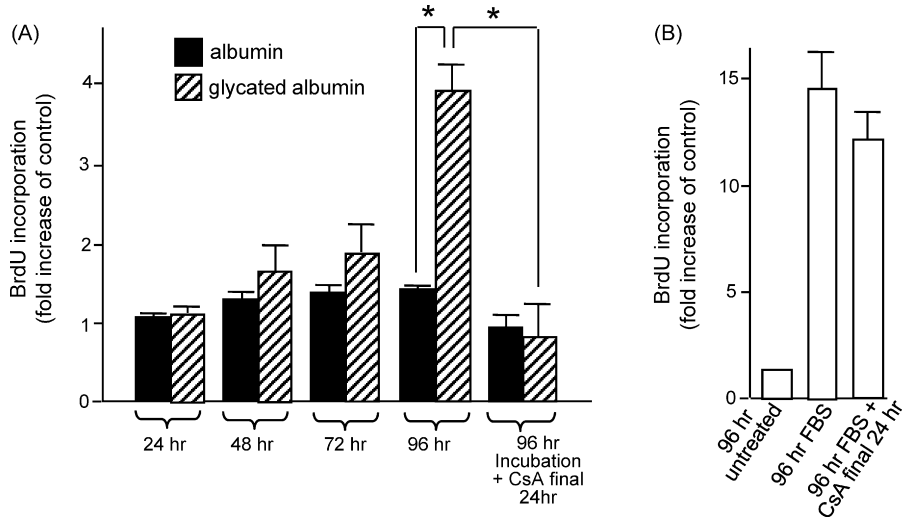

Fig. 6 – BrdU incorporation in cells preincubated with AGE. (A) Cells were preincubated for 24, 48, 72 or 96 h either untreated (not shown), with 200 μg/ml albumin or 200 μg/ml glycated albumin and BrdU incorporation was measured. Some experiments using 96 h incubation included 10 μM CsA for the final 24 h of the 96 h incubation. (B) BrdU incorporation in cells incubated with 10% FBS for 96 h with CsA for the final 24 h of the 96 h incubation. $n = 4$ for each group, $^{*}p < 0.05$. Each experiment was conducted using cells derived from different animals.

4. Discussion

Evidence now indicates that the production of AGEs in the hyperglycaemic environment of diabetes could have an important role in the development of atherosclerosis. Atherosclerosis involves a switch to a more proliferative VSM cell phenotype. AGE can induce VSM cell proliferation although the mechanisms are not clear. In this study, glycated albumin at a concentration which reflects that found *in vivo* [41] produced a prolonged agonist-induced Ca^{2+} rise in VSM cells. This is at least partly attributable to an increase in the ryanodine-sensitive component involved in Ca^{2+}-induced Ca^{2+} release from the sarcoplasmic reticulum. Prolongation of the Ca^{2+} increase resulted in increased activation of the Ca^{2+}-dependent phosphatase, calcineurin, and subsequent activation of NFATc. This regulation of NFATc is possibly involved in the AGE-induced proliferation previously observed in VSM cells and may contribute *in vivo* to vascular changes associated with hyperglycaemia.

The present study has used glycated albumin as an example of AGEs found *in vivo*, and closely associated with diabetic vascular complications [46,47]. Many studies have used this AGE to investigate mechanisms of AGE-induced signaling (e.g. [23,24,31]). Glycated albumin does bind and activate RAGE [48]. Although some questions remain to be answered regarding the applicability of glycated proteins prepared *in vitro* (such as the degree of modification of the protein compared to that produced *in vivo* [49]), glycated albumin is a useful tool to analyse potential RAGE-mediated signaling pathways. In VSM cells, previous studies have demonstrated activation, via RAGE, of various pathways including MAPK kinase isoforms with shorter incubation times [24]. In our study, we have used longer-term (96 h) incubation with AGE to better assess chronic effects on VSM cells. This is particularly relevant to the *in vivo* situation in diabetes where arteries are chronically exposed to AGEs, including glycated albumin. Such incubation would be expected to result in changes to protein expression. As has previously been reported in endothelial cells [50], RAGE expression in this study shows a significant increase following incubation with AGE. In addition, RAGE expression in VSM cells is upregulated during vascular injury [34]. This increased expression could account for an increase in AGE-RAGE signaling and does demonstrate that this receptor pathway is present in these cells. We have not directly demonstrated that RAGE signaling is involved in this mechanism, for example by utilizing RAGE antagonists such as soluble RAGE or RAGE −/− cells. However, glycated albumin does activate ERK1/2, a known effector of RAGE signaling, in cultured pig coronary artery VSM cells previously characterized by others [32]. This provides some indirect evidence that AGE effects are mediated via RAGE in this study. Further experiments will be required to definitely show the involvement of RAGE.

Ca^{2+}-dependent signaling is critical for normal cell function and alterations to these pathways can have dramatic effects on cell phenotype. In the case of AGE incubation in VSM cells as shown in this study, effects on Ca^{2+} signaling may contribute to a more proliferative phenotype. This change in Ca^{2+} signaling results in an agonist-induced Ca^{2+} rise which is of significantly longer duration; approximately double that of control responses. The peak Ca^{2+} increase is not altered. This is reflected in results from both Ca^{2+} imaging and from electrophysiology where the prolonged inward current is Ca^{2+} activated [42]. These findings are in agreement with a previous study in VSM cells isolated from diabetic patients which found that the agonist-induced Ca^{2+} increase was enhanced, particularly at the perinuclear region suggesting release from intracellular stores [51]. The Ca^{2+} increase induced by the

agonist used in this study (S1P) is predominantly the result of release from intracellular stores in VSM cells [42], involving IP_3-induced calcium release (via IP_3 receptors) and to a lesser extent Ca^{2+}-induced Ca^{2+} release (CICR) via ryanodine receptors (RyR). The photolysis of caged IP_3 and caged Ca^{2+} demonstrate that effects of S1P in AGE-treated cells are not agonist specific but are likely to be observed by any agonist that increases IP_3 or intracellular Ca^{2+}. This shows the broad nature of the modulation of Ca^{2+} signaling that occurs following AGE incubation. Interestingly, an inhibition of CICR by ryanodine following 96 h AGE incubation reduces slightly the peak Ca^{2+} rise, but also completely abolishes the prolonged duration of this rise. The involvement of RyR is further indicated by the effects of caffeine following AGE incubation, which results in an increased peak Ca^{2+} rise and prolonged duration. These results are also reflected in electrophysiological experiments using caged Ca^{2+} (DM-nitrophen). In VSM cells pre-incubated with AGE, there is a significantly greater inward current evoked following photolysis compared to control cells indicating an increased CICR mechanism. The exact nature of this change in the RyR-dependent Ca^{2+} homeostasis is not yet clear. Changes in either RyR expression or channel regulation may explain the altered Ca^{2+} homeostasis. Three RyR isoforms, RyR1, RyR2 and RyR3, have been cloned and characterized [52]. Although RyR3 is typically associated with VSM cells, some smooth muscles express all three isoforms [53]. Promoter sites regulating RyR gene expression are not yet resolved. Further detailed study will be required to determine the nature of this altered CICR by AGE. The additional involvement of other pathways in this AGE-induced mechanism can also not be excluded, such as altered activity of Ca^{2+}-ATPases, particularly as the observed effects result in a prolonged duration of the Ca^{2+} increase, and will require further detailed investigation.

The changes in the agonist-induced Ca^{2+} increase as a result of AGE incubation would be expected to have downstream effects on VSM cell function. Indeed, in this study we have demonstrated that a Ca^{2+}-dependent pathway which likely has a role in regulating cell phenotype, namely CaN/NFATc [44,45], is regulated as a result of these changes. The prolonged agonist-induced Ca^{2+} increase observed following 96 h AGE incubation results in an increased activation of the Ca^{2+}/calmodulin-dependent phosphatase, CaN, measured after 30 min of agonist stimulation. In addition, the basal levels of CaN are increased by AGE incubation for 96 h directly indicating an elevated resting $[Ca^{2+}]_i$. Although the fluorescence Ca^{2+} imaging did not reflect an increased basal resting Ca^{2+}, the arbitrary ratio units of measurement used would not detect any small changes of this parameter. CaN is a protein phosphatase 2B with several downstream targets, including the transcription factor family, NFATc [41]. NFATc consists of five isoforms, NFATc1, NFATc2 and NFATc3 present in VSM cells [44]. NFATc resides in the cytoplasm in a hyperphosphorylated state. Dephosphorylation by CaN exposes nuclear localization domains which target NFATc to the nucleus and initiate NFAT-induced gene expression [43]. In the present study, AGE preincubation results in an increase in both basal and agonist-stimulated NFATc activation, reflecting the increase in CaN activation. Persistent activation of CaN is required to maintain NFATc activation [54]. The increased resting Ca^{2+} level, as well as the prolonged agonist-induced Ca^{2+} rise observed following AGE preincubation, are likely to contribute to the increased basal activation and enhanced agonist-stimulated activation of NFATc. This maintained effect will push towards a phenotypic alteration in VSM cells chronically exposed to AGE.

NFATc has been implicated in having an important role in VSM proliferation related to vascular disease [45,55] although the exact nature of NFATc-induced gene expression which contributes to this is not clear. This may be via an upregulation of inflammatory factors such as interleukin-6 or COX-2 [56,57]. Reports have suggested that NFATc may also be involved in smooth muscle-specific gene expression during vascular development via interaction with GATA transcription factors [58], tending to point to a role in differentiation rather than proliferation in some circumstances. Regardless, several studies have indicated that blockade of NFATc activation does prevent VSM proliferation *in vitro* and inhibit neointimal growth *in vivo* suggesting the importance of NFATc regulation in the development of vascular disease [45,55,57]. Previous studies have also demonstrated that AGEs can induce proliferation in VSM cells [23,24] although the intracellular mechanisms are not clear. The present study demonstrates that at least part of the AGE-induced proliferation is due to activation of NFATc as it is blocked by CsA, a selective inhibitor of the CaN/NFATc pathway. When CsA is added 72 h after proliferation has been initiated by AGE, BrdU incorporation is still significantly decreased compared to control-treated cells. This timecourse fits well with the observed timecourse of the increased basal and agonist-stimulated CaN activation following AGE incubation. This is also in line with the AGE-induced increase in the duration of agonist-stimulated Ca^{2+} increase. Further evidence that the NFATc pathway is selective for AGE-induced proliferation (as opposed to a different mitogenic stimulus), is demonstrated by the lack of effect of CsA in blocking serum-induced proliferation under the same condition. Although serum incubation represents a powerful mitogenic stimulus activating many pathways, it does suggest that inhibition of NFATc activation is not necessarily always sufficient for proliferation, but is required for AGE-induced proliferation. It is acknowledged that a short incubation with AGE does activate ERK1/2 in VSM cells [23,24] and may also initiate proliferation via other pathways in addition to the CaN/NFATc-dependent pathway demonstrated by the present study. However, at least after 72–96 h of AGE incubation (more accurately reflecting the chronic exposure observed *in vivo*), this mechanism could play an important role in maintaining the proliferation.

In conclusion, VSM cells preincubated with AGE for 96 h demonstrate an altered Ca^{2+} homeostasis. This alteration involves a change in the CICR resulting in a prolonged agonist-induced increase in $[Ca^{2+}]_i$. The prolonged elevation of $[Ca^{2+}]_i$ leads to increased activation of the Ca^{2+}/calmodulin-dependent protein phosphatase, CaN, and subsequently increased activation of the transcription factor, NFATc. NFATc is, at least partly, required for AGE-induced proliferation in VSM cells. Therefore, in conditions of high circulating glucose concentrations, such as diabetes, this mechanism may contribute to the development of vascular disease.

Acknowledgments

KCD was supported by a Fernando Fellowship. The authors would like to thank Irene Hunter for invaluable technical assistance.

REFERENCES

[1] Hanssen KF. Blood glucose control and microvascular and macrovascular complications. Diabetes 1997;46:S101–3.
[2] The Diabetes Control and Complications Trial Research Group. The effect of intensive treatment of diabetes on the development and progression of long-term complications in insulin-dependent diabetes mellitus. N Eng J Med 1993;329:977–86.
[3] Beckman JA, Creager MA, Libby P. Diabetes and atherosclerosis: epidemiology, pathophysiology, and management. JAMA 2002;287:2570–81.
[4] Brownlee M. Biochemistry and molecular cell biology of diabetic complications. Nature 2001;414:813–9.
[5] Cameron NE, Cotter MA, Basso M, Hohman TC. Comparison of the effects of inhibitors of aldose reductase and sorbitol dehydrogenase on neurovascular function, nerve conduction and tissue polyol pathway metabolites in streptozotocin-diabetic rats. Diabetologia 1997;40:271–81.
[6] Lee AY, Chung SS. Contributions of polyol pathway to oxidative stress in diabetic cataract. FASEB J 1999;13:23–30.
[7] Kuboki K, Jiang ZY, Takahara N, Ha SW, Igarashi M, Yamauchi T, et al. Regulation of endothelial constitutive nitric oxide synthase gene expression in endothelial cells and in vivo: a specific vascular action of insulin. Circulation 2000;101:676–81.
[8] Sayeski PP, Kudlow JE. Glucose metabolism to glucosamine is necessary for glucose stimulation of transforming growth factor-α gene transcription. J Biol Chem 1996;271:15237–43.
[9] Wells L, Hart G. O-GlcNAc turns twenty: functional implications for posttranslational modification of nuclear and cytosolic protein with a sugar. FEBS Lett 2003;546: 154–8.
[10] Goldin A, Beckman JA, Schmidt AM, Creager MA. Advanced glycation end products: sparking the development of diabetic vascular injury. Circulation 2006;114:597–605.
[11] Hudson BI, Wendt T, Bucciarelli LG, Rong LL, Naka Y, Yan SF, Schmidt AM. Diabetic vascular disease: it's all the RAGE. Antioxid Redox Signal 2005;7:1588–600.
[12] Thomas MC, Baynes JW, Thorpe SR, Cooper ME. The role of AGEs and AGE inhibitors in diabetic cardiovascular disease. Curr Drug Targets 2005;6:453–74.
[13] Thornalley PJ. The glyoxalase system: new developments towards functional characterization of a metabolic pathway fundamental to biological life. Biochem J 1990;269:1–11.
[14] Baynes JW, Thorpe SR. Role of oxidative stress in diabetic complications: a new perspective on an old paradigm. Diabetes 1999;48:1–9.
[15] Lyon T, Jenkins AJ. Glycation, oxidation and lipoxidation in the development of the complications of diabetes mellitus; a carbonyl stress hypothesis. Diabetes Rev 1997;5: 365–91.
[16] Ahmed N, Thornalley PJ. Advanced glycation endproducts: what is their relevance to diabetic complications? Diabetes Obes Metab 2007;9:233–45.
[17] Jakus V, Reitbrock N. Advanced glycation end-products and the progress of diabetic vascular complications. Physiol Res 2004;53:131–42.
[18] Berg TJ, Dahl-Jorgensen K, Torjesen PA, Hanssen KF. Increased serum levels of advanced glycation endproducts in children and adolescents with IDDM. Diabetes Care 1997;20:1006–8.
[19] Nakamura S, Makita Z, Ishikawa S, Yasumura K, Fujii W, Yanagisawa K, et al. Progression of nephropathy in spontaneous diabetic rats is prevented by OPB-9195, a novel inhibitor of advanced glycation. Diabetes 1997;46:895–9.
[20] Hammes HP, Martin S, Federlin K, Geisen K, Brownlee M. Aminoguanidine treatment inhibits the development of experimental diabetic retinopathy. Proc Natl Acad Sci USA 1991;88:11555–9.
[21] Zhou Z, Wang K, Penn MS, Marso SP, Lauer MA, Forudi F, et al. Receptor for AGE (RAGE) mediates neointimal formation in response to arterial injury. Circulation 2003;107:2238–43.
[22] Kislinger T, Tanji N, Wendt T, Qu W, Lu Y, Ferran Jr LJ, et al. Receptor for advanced glycation end products mediates inflammation and enhanced expression of tissue factor in vasculature of diabetic apolipoprotein E-null mice. Arterioscler Thromb Vasc Biol 2001;21:905–10.
[23] Satoh H, Togo M, Hara M, Miyata T, Han K, Maekawa H, et al. Advanced glycation endproducts stimulate mitogen-activated protein kinase and proliferation in rabbit vascular smooth muscle cells. Biochem Biophys Res Commun 1997;239:111–5.
[24] Hattori Y, Suzuki M, Hattori S, Kasai K. Vascular smooth muscle cell activation by glycated albumin (Amadori adducts). Hypertension 2002;39:22–8.
[25] Neeper M, Schmidt AM, Brett J, Yan SD, Wang F, Pan YC, et al. Cloning and expression of a cell surface receptor for advanced glycosylation end products of proteins. J Biol Chem 1992;267:14998–5004.
[26] Brett J, Schmidt AM, Yan SD, Zou YS, Weidman E, Pinsky D, et al. Survey of the distribution of a newly characterized receptor for advanced glycation end products in tissues. Am J Pathol 1993;143:1699–712.
[27] Schmidt AM, Yan SD, Yan SF, Stern DM. The multiligand receptor RAGE as a progression factor amplifying immune and inflammatory responses. J Clin Invest 2001;108:949–55.
[28] Yonekura H, Yamamoto Y, Sakurai S, Petrova RG, Abedin MJ, Li H, et al. Novel splice variants of the receptor for advanced glycation end-products expressed in human vascular endothelial cells and pericytes, and their putative roles in diabetes-induced vascular injury. Biochem J 2003;370:1097–109.
[29] Bierhaus A, Humpert PM, Morcos M, Wendt T, Chavakis T, Arnold B, et al. Understanding RAGE, the receptor for advanced glycation end products. J Mol Med 2005;83:876–86.
[30] Schiekofer S, Andrassy M, Chen J, Rudofsky G, Schneider J, Wendt T, et al. Acute hyperglycemia causes intracellular formation of CML and activation of ras, p42/44 MAPK, and nuclear factor kappaB in PBMCs. Diabetes 2003;52:621–33.
[31] Bierhaus A, Illmer T, Kasper M, Luther T, Quehenberger P, Tritschler H, et al. Advanced glycation end product (AGE)-mediated induction of tissue factor in cultured endothelial cells is dependent on RAGE. Circulation 1997;96:2262–71.
[32] Lander HM, Tauras JM, Ogiste JS, Hori O, Moss RA, Schmidt AM. Activation of the receptor for advanced glycation endproducts triggers a $p21^{ras}$-dependent mitogen-activated protein kinase pathway regulated by oxidant stress. J Biol Chem 1997;272:17810–4.
[33] Park L, Raman KG, Lee KJ, Lu Y, Ferran Jr LJ, Chow WS, et al. Suppression of accelerated diabetic atherosclerosis by the soluble receptor for advanced glycation endproducts. Nat Med 1998;4:1025–31.
[34] Sakaguchi T, Yan SF, Yan SD, Belov D, Rong LL, Sousa M, et al. Central role of RAGE-dependent neointimal

expansion in arterial restenosis. J Clin Invest 2003;111: 959–72.
[35] Cartin L, Lounsbury KM, Nelson MT. Coupling of Ca^{2+} to CREB activation and gene expression in intact cerebral arteries from mouse. Circ Res 2000;86:760–7.
[36] Lipskaia L, Lompre AM. Alteration in temporal kinetics of Ca^{2+} signaling and control of growth and proliferation. Biol Cell 2004;96:55–68.
[37] Egan CG, Wainwright CL, Wadsworth RM, Nixon GF. PDGF-induced signaling in proliferating and differentiated vascular smooth muscle: effects of altered intracellular Ca^{2+} regulation. Cardiovasc Res 2005;67:308–16.
[38] Petrova R, Yamamoto Y, Muraki K, Yonekura H, Sakurai S, Watanabe T, et al. Advanced glycation endproduct-induced calcium handling impairment in mouse cardiac myocytes. J Mol Cell Cardiol 2002;34:1425–31.
[39] Currie KPM, Wootton JF, Scott RH. Activation of Ca^{2+}-dependent Cl^- currents in cultured rat sensory neurones by flash photolysis of DM-nitrophen. J Physiol 1995;482:291–307.
[40] Zhang L, Zalewski A, Liu Y, Mazurek T, Cowan S, Martin JL, et al. Diabetes-induced oxidative stress and low-grade inflammation in porcine coronary arteries. Circulation 2003;108:472–8.
[41] Negoro H, Morley JE, Rosenthal MJ. Utility of serum fructosamine as a measure of glycemia in young and old diabetic and non-diabetic subjects. Am J Med 1988;85:360–4.
[42] Coussin F, Scott RH, Wise A, Nixon GF. Comparison of sphingosine 1-phosphate-induced intracellular signaling pathways in vascular smooth muscles: differential role in vasoconstriction. Circ Res 2002;91:151–7.
[43] Tones MA, Bootman MD, Higgins BF, Lane DA, Pay GF, Lindahl U. The effect of heparin on the inositol 1,4,5-trisphosphate receptor in rat liver microsomes. FEBS Lett 1989;252:105–8.
[44] Hogan PG, Chen L, Nardone J, Rao A. Transcriptional regulation by calcium, calcineurin, and NFAT. Genes Dev 2003;17:2205–32.
[45] Yellaturu CR, Ghosh SK, Rao RK, Jennings LK, Hassid A, Rao GN. A potential role for nuclear factor of activated T-cells in receptor tyrosine kinase and G-protein-coupled receptor agonist-induced cell proliferation. Biochem J 2002;368: 183–90.
[46] Cohen MP, Clements RS, Cohen JA, Shearman CW. Glycated albumin promotes a generalized vasculopathy in the db/db mouse. Biochem Biophys Res Commun 1996;218:72–5.
[47] Clements Jr RS, Robison Jr WG, Cohen MP. Anti-glycated albumin therapy ameliorates early retinal microvascular pathology in db/db mice. J Diabetes Complicat 1998;12: 28–33.
[48] Valencia JV, Weldon SC, Quinn D, Kiers GH, DeGroot J, TeKoppele JM, et al. Advanced glycation end product ligands for the receptor for advanced glycation end products: biochemical characterization and formation kinetics. Anal Biochem 2004;324:68–78.
[49] Ramasamy R, Yan SF, Schmidt AM. Arguing for the motion: yes, RAGE is a receptor for advanced glycation endproducts. Mol Nutr Food Res 2007;51:1111–5.
[50] Tanaka N, Yonekura H, Yamagishi S, Fujimori H, Yamamoto Y, Yamamoto H. The receptor for advanced glycation end products is induced by the glycation products themselves and tumor necrosis factor-alpha through nuclear factor-kappa B, and by 17beta-estradiol through Sp-1 in human vascular endothelial cells. J Biol Chem 2000;275:25781–90.
[51] Fleischhacker E, Esenabhalu VE, Spitaler M, Holzmann S, Skrabal F, Koidl B, Kostner GM, Graier WF. Human diabetes is associated with hyperreactivity of vascular smooth muscle cells due to altered subcellular Ca^{2+} distribution. Diabetes 1999;48:1323–30.
[52] Rossi D, Sorrentino V. Molecular genetics of ryanodine receptors Ca^{2+}-release channels. Cell Calcium 2002;32: 307–19.
[53] Kinnear NP, Wyatt CN, Clark JH, Calcraft PJ, Fleischer S, Jeyakumar LH, et al. Lysosomes co-localize with ryanodine receptor subtype 3 to form a trigger zone for calcium signalling by NAADP in rat pulmonary arterial smooth muscle. Cell Calcium 2008;44:190–201.
[54] Timmerman LA, Clipstone NA, Ho SN, Northrop JP, Crabtree GR. Rapid shuttling of NF-AT in discrimination of Ca^{2+} signals and immunosuppression. Nature 1996;383:837–40.
[55] Yu H, Sliedregt-Bol K, Overkleeft H, van der Marel GA, van Berkel TJ, Biessen EA. Therapeutic potential of a synthetic peptide inhibitor of nuclear factor of activated T cells as antirestenotic agent. Arterioscler Thromb Vasc Biol 2006;26:1531–7.
[56] Nilsson LM, Sun ZW, Nilsson J, Nordström I, Chen YW, Molkentin JD, et al. Novel blocker of NFAT activation inhibits IL-6 production in human myometrial arteries and reduces vascular smooth muscle cell proliferation. Am J Physiol Cell Physiol 2007;292:C1167–78.
[57] Liu Z, Zhang C, Dronadula N, Li Q, Rao GN. Blockade of nuclear factor of activated T cells activation signaling suppresses balloon injury-induced neointima formation in a rat carotid artery model. J Biol Chem 2005;280:14700–8.
[58] Wada H, Hasegawa K, Morimoto T, Kakita T, Yanazume T, Abe M, et al. Calcineurin-GATA-6 pathway is involved in smooth muscle-specific transcription. J Cell Biol 2002;156:983–91.